Direct Kinetic Studies of Reactions of 3-Pentoxy Radicals with NO and O_2

Wei Deng, Andrew J. Davis, Lei Zhang, David R. Katz, and Theodore S. Dibble*

Department of Chemistry, State University of New York, College of Environmental Science and Forestry, 1 Forestry Drive, Syracuse, New York 13210

Received: May 15, 2001; In Final Form: July 26, 2001

Kinetic studies of the reactions of 3-pentoxy with NO and O_2 have been performed using laser-induced fluorescence detection of 3-pentoxy radicals. Experiments were carried out at a total pressure of 50 Torr at subambient temperatures. Arrhenius expressions are obtained for the reactions of 3-pentoxy with NO (k_{NO}) and O_2 (k_{O_2}): $k_{NO} = (5.6 \pm 1.6) \times 10^{-13} \exp[(7.8 \pm 0.6)\ \text{kJ mol}^{-1}/RT]\ \text{cm}^3\ \text{molecule}^{-1}\ \text{s}^{-1}$ (216−276 K), and $k_{O_2} = (4.1 \pm 1.2) \times 10^{-15} \exp[(2.6 \pm 0.6)\ \text{kJ mol}^{-1}/RT]\ \text{cm}^3\ \text{molecule}^{-1}\ \text{s}^{-1}$ (220−285 K). No pressure dependence was observed for either rate constant at 243 K between 50 and 150 Torr. The negative temperature dependence of k_{NO} is significantly larger than that of other alkoxy radicals, and this suggests a 298 K rate constant that is only one-third to half those measured for other alkoxy radicals. The small negative temperature dependence of k_{O_2} is different from the small positive temperature dependence observed for ethoxy and propoxy radicals but is comparable to that previously observed for 2-butoxy radicals. The observed temperature dependencies of k_{NO} and k_{O_2} confound expectations that the kinetics of the reactions of larger alkoxy radicals would be very similar to the kinetics of C_1-C_3 alkoxy radicals.

I. Introduction

The formation of ozone and secondary organic aerosol in polluted air results from the gas-phase oxidation of volatile organic compounds (VOC) in the presence of solar radiation.[1] Alkoxy radicals are very important reaction intermediates in VOC oxidation. It is well-known that three competing reaction pathways dominate the fate of large alkoxy radicals: decomposition, reaction with O_2, and isomerization.[2,3] Each reaction channel has potentially different effects on the yields of ozone and secondary organic aerosol formed during a smog episode. Although alkoxy radical + NO reactions are rarely significant under atmospheric conditions, they are commonly used as reference reactions in relative rate studies of alkoxy radical kinetics.[3] Relatively few absolute rate constants are known for alkoxy radical reactions, and the data are even scantier for large alkoxy radicals ($\geq C_4$). The modeling of tropospheric phenomena requires a good understanding of alkoxy radical chemistry; however, the absence of kinetic data for large alkoxy radicals undermines the reliability of such efforts. The present understanding of large alkoxy radicals is primarily based on product-yield and relative-rate studies,[3] quantum calculations,[4−6] and real-time monitoring of OH and NO_2 in cycling experiments.[7−9]

Laser-induced fluorescence (LIF) spectroscopy long ago demonstrated its ability in monitoring C_1-C_3 alkoxy radicals for direct studies of reaction kinetics.[10−20] Spectra of larger alkoxy radicals have only been investigated recently[21−23] and used for kinetic studies by ourselves[24] and others.[21,25−27] Jet-cooled LIF spectra, recently obtained by Carter et al., tend to confirm the previous identification of these larger alkoxy radicals and extend our knowledge to alkoxy radicals containing up to 12 carbon atoms.[28,29]

Hein et al. monitored OH cycling and NO_2 formation to determine the absolute rate constants of unimolecular and bimolecular reactions of 2-butoxy, 1-butoxy, 1-pentoxy, and 3-pentoxy.[7−9] However, all of the experiments were carried out at 293 K, so the activation barriers were not obtained. Moreover, these studies used a somewhat indirect method: extracting the rate constants depended on the reliable understanding of a complex reaction scheme. To date, direct kinetic studies have only been carried out for the unimolecular decomposition of *tert*-butoxy radicals,[21,25] its reactions with NO and NO_2,[21,26] and the reactions of 2-butoxy radicals with NO, O_2, and NO_2.[24,27]

In this paper, we have investigated the temperature dependence of the rate constants for the reactions of a five-carbon-atom alkoxy radical, namely, 3-pentoxy, with NO and O_2 and using the direct detection of 3-pentoxy by LIF. Arrhenius expressions for the rates of both reactions are acquired for the first time.

II. Experimental Section

3-Pentyl nitrite was produced by the dropwise addition of sulfuric acid to a mixture of 3-pentanol and sodium nitrite.[30] Purification was performed by freeze−pump−thaw cycles followed by trap-to-trap distillation. The identity and purity of 3-pentyl nitrite were verified by its FTIR,[31] UV,[32] and NMR[31] spectra. 3-Pentyl nitrite was then diluted in nitrogen to a mole fraction of 0.02 and stored in a 10 L darkened gas bulb.

The reaction cell (1.4 L) consists of a Pyrex tube with two long glass side arms containing apertures and quartz windows attached at Brewster's angles. A frequency-tripled Nd:YAG laser (Quanta-Ray DCR-2) provides a ~15 mJ/pulse at 355 nm for the photolysis of 3-pentyl nitrite. To minimize secondary chemistry, we modified the experiment by not focusing the photolysis laser beam and introducing it to the cell at 90° relative to the probe beam (through a side window into the reaction cell). The probe beam from an excimer-pumped dye laser (Lambda Physik Lextra 100 and FL 3002) passes through the long arms of the cell. The probe laser is operated at 3.3 Hz with a pulse energy of 1−2 mJ. The 3-pentoxy radicals are

* To whom correspondence should be addressed. E-mail: tsdibble@syr.edu. Fax: (315) 470-6856.

10.1021/jp011875i CCC: $20.00
Published on Web 09/08/2001

probed by monitoring the fluorescence resulting from the excitation of $\tilde{B} \rightarrow \tilde{X}$ (2−0) transition at 362.9 nm.

The fluorescence signal is collected perpendicularly to the laser beams and normalized by dividing by the signal obtained from a photodiode (Thorlabs DET 200) exposed to the light scattered from the optics train of the probe beam. A cutoff filter (CVI Laser LP-435) was used to reduce the scattered light. The delay time between the two lasers was varied between 5 and 500 μs. At each delay time, 200 points were averaged. We treated the LIF signal at the delay time of 500 μs as the background signal on the basis of empirical observations that the LIF signal was lower at this time than at shorter or longer times. The background signal was subtracted from the signal obtained at each delay time to construct the decay curve.

To avoid the accumulation of photolysis or reaction products between the successive laser pulses, 2% 3-pentyl nitrite in nitrogen flows continuously through the reaction cell at 20 sccm. The residence time of the gas in the cell is about 20 s. We verified that 3-pentyl nitrite is unreactive with the walls of the cell by letting a sample of 2% 3-pentyl nitrite sit in the cell for 20 min. A portion of the mixture was then analyzed by FTIR. No peaks were observed other than those attributable to 3-pentyl nitrite, indicating that no significant wall reaction occurs. The absence of gas-phase and wall reactions of 3-pentyl nitrite with O_2 and NO was verified in the same manner. Calibrated flow controllers (MKS 247) are used to control the flow rates of the nitrite−gas mixture and the NO or O_2. The concentration of each gas in the reaction cell was calculated from the total pressure, as determined by a capacitance manometer (MKS 662), and their mole fractions. The flow of the nitrogen buffer gas is controlled manually by adjusting a needle valve. Typical concentrations of the reactants were as follows: 3-pentyl nitrite, $(4-5) \times 10^{15}$ molecules cm^{-3}; NO, $(1-5) \times 10^{15}$ molecules cm^{-3}; O_2, $(1-10) \times 10^{17}$ molecules cm^{-3}. Using the 355 nm absorption cross section of 3-pentyl nitrite measured in our laboratory (1.4×10^{-19} cm^2 molecules^{-1}) and the diameter of the photolysis laser beam (0.4 cm), we are able to estimate that the photolysis pulse produces an initial 3-pentoxy concentration of 5×10^{13} molecules cm^{-3}.

The carrier gas (N_2, MG 99.999%) and the reactants NO (Matheson 99.0%; a mixture of 0.0092 mole fraction in N_2, 99.9%) and O_2 (MG 99.999%) are used without further purification. The total pressure inside the reaction cell was typically maintained at 50 Torr. The temperature inside the reaction cell is measured by a thermocouple located directly below the reaction zone. The temperature range was controlled between 216 and 285 K by adjusting the temperature of circulating ethanol from a thermostated bath through the jacket surrounding the reaction cell. The degradation in the structure of the LIF excitation spectrum of 3-pentoxy as the temperature increases limits the upper temperature range accessible with the present apparatus.

III. Results and Discussion

1. Reaction of 3-Pentoxy with NO. Typical 3-pentoxy LIF signal decay curves as a function of delay time are shown in Figure 1. The pseudo-first-order approximation allows us to obtain the bimolecular rate constants of the 3-pentoxy + NO reaction, k_{NO}, from the slopes of the plots of the pseudo-first-order rate constants against the concentration of NO (as in Figure 2). As illustrated in Figure 3, values of k_{NO} decrease by a factor of 3 as the temperature is increased from 216 to 276 K, from 4.5×10^{-11} to 1.6×10^{-11} cm^3 molecule^{-1} s^{-1}, respectively. An Arrhenius expression for the temperature dependence of the rate constants can be derived from a plot of ln(k_{NO}) versus 1/T:

$$k_{NO} = (5.62 \pm 1.62) \times 10^{-13} \exp[(7.84 \pm 0.58)\ \text{kJ mol}^{-1}/RT]\ \text{cm}^3\ \text{molecule}^{-1}\ \text{s}^{-1}$$

(All uncertainties reported in this paper represent a statistical 1σ error, unless otherwise specified). Table 1 summarizes the literature on the kinetics of alkoxy radical reactions with NO. The reactions of propoxy and butoxy radical isomers with NO all have nearly the same activation energy (E_a) of about −3 kJ mol^{-1}, but 3-pentoxy has a much more negative activation energy (−7.8 kJ mol^{-1}). The Arrhenius pre-exponential factor

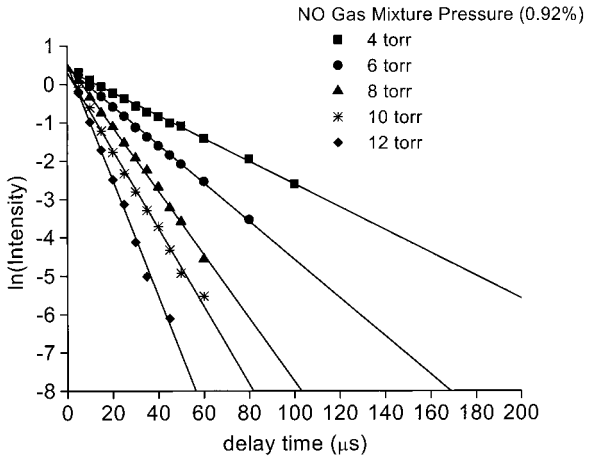

Figure 1. Typical LIF intensity versus time profiles for 3-pentoxy in the presence of different pressures of an NO gas mixture (0.92% in nitrogen) at 224 K: (◆) 12 Torr, (*) 10 Torr, (▲) 8 Torr, (●) 6 Torr, and (■) 4 Torr; solid lines represent the best fits.

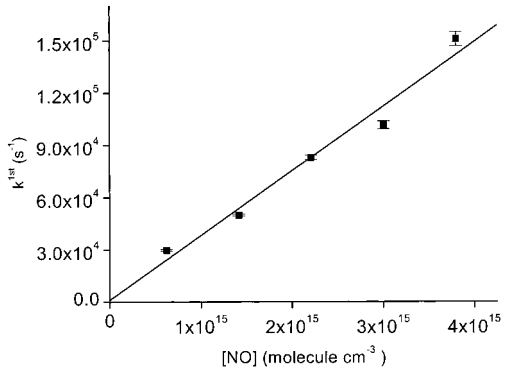

Figure 2. Plot of the pseudo-first-order rate constant versus the NO concentration at 224 K.

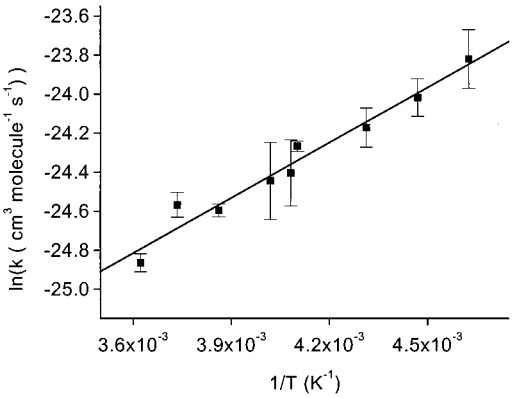

Figure 3. Arrhenius plot showing the negative temperature dependence of the rate constant for the reaction of 3-pentoxy with NO.

TABLE 1: Arrhenius Parameters from Direct Studies of the Reaction of Alkoxy Radicals with NO

radical	A (cm^3 molecule^{-1} s^{-1})	E_a (kJ mol^{-1})	temp range (K)	ref
C_2H_5O	2.0×10^{-11}	−0.6	286−388	14
1-C_3H_7O	1.2×10^{-11}	−2.9	289−380	20
2-C_3H_7O	1.22×10^{-11}	−2.6	298−383	13
	0.89×10^{-11}	−3.3	286−380	20
tert-C_4H_9O	0.78×10^{-11}	−2.85	200−390	21
	0.76×10^{-11}	−3.2	223−305	26
2-C_4H_9O	0.75×10^{-11}	−2.98	223−311	24
	0.91×10^{-11}	−3.4	223−305	27
3-pentoxy	0.056×10^{-11}	−7.84	216−276	this work
all ≥C_4	2.3×10^{-11}	−1.25		3

is also much lower than that for other alkoxy radicals. The Arrhenius expression can be extrapolated to obtain the rate constant at room temperature, $k_{298K} = (1.3 \pm 0.5) \times 10^{-11}$ cm^3 molecule^{-1} s^{-1}. This is significantly smaller than Atkinson's recommended value of 3.8×10^{-11} cm^3 molecule^{-1} s^{-1}.[2,3]

The reaction of secondary alkoxy radicals with NO is generally believed to proceed through two channels: the addition of NO and the abstraction of an α-hydrogen atom. The addition channel is thought to dominate in all but the lowest pressures.[2,15] Because we measured the disappearance of 3-pentoxy radicals, the rate constant we obtained is the sum of parts a and b of eq 1.

$$CH_3CH_2CH(O\bullet)CH_2CH_3 + NO \rightarrow CH_3CH_2CH(ONO)CH_2CH_3 \quad (1a)$$

$$\rightarrow CH_3CH_2C(=O)CH_2CH_3 + HNO \quad (1b)$$

However, Caralp et al. have proposed a barrierless pathway to HNO formation from $CH_3O + NO$,[33] and such a change in mechanism might explain the very different activation energy observed here. A test of the pressure dependence of k_{NO} was carried out within the pressure range P(total) = 50−150 Torr at 243 K. No significant pressure effect was observed. Previous experiments suggested that the reactions of ethoxy[14] and propoxy[20] with NO approach the high-pressure limit by 15 and 30 Torr, respectively, and no pressure dependence was found for the reactions of NO with *tert*-butoxy[21] and 2-butoxy in the pressure ranges of 5−80 and 7−175 Torr, respectively.[24,27] The lack of any pressure dependence in the present study is consistent with these observations.

Rate constants appear to be insensitive to the energy of the photolysis laser pulse and the flow rate of the gases. Upon reducing the power of the photolysis laser by 56% at 243 K and the total pressure by 50 Torr, we obtained a rate constant k_{243K} of $(2.2 \pm 0.4) \times 10^{-11}$ cm^3 molecule^{-1} s^{-1}, which agrees within the experimental uncertainty with the value of $(2.7 \pm 0.5) \times 10^{-11}$ cm^3 molecule^{-1} s^{-1} calculated from the Arrhenius expression. The flow rates of all of the gases were doubled while keeping their partial pressures constant; the rate constant obtained, $(2.6 \pm 0.1) \times 10^{-11}$ cm^3 molecule^{-1} s^{-1}, was nearly identical to the calculated value.

The statistical uncertainties in the individual rate constants are not the only source of error in determining the rate constants or the Arrhenius parameters. Potential errors in determining NO concentrations (5%) generate a 5% error in the computed rate constants at a given temperature. The temperature measurements contain a 1% calibration error and a potential for another 1% error (overestimate) of the temperature because the thermocouple is located slightly below the reaction zone in a warmer part of the gas flow. We measured an NO_2 impurity in the NO at the level of about 1% of the NO concentration; however, this is unlikely to have a significant effect on the rate constants.[27] We therefore estimate the true 2σ uncertainty in the computed activation energy as about 20%.

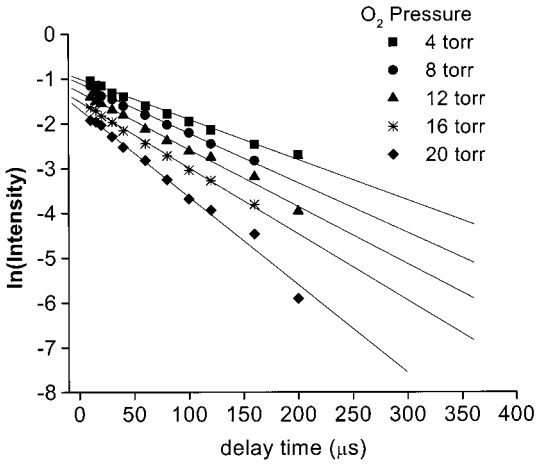

Figure 4. Typical LIF intensity versus time profiles for 3-pentoxy in the presence of different pressures of O_2 at 224 K: (◆) 20 Torr, (*) 16 Torr, (▲) 12 Torr, (●) 8 Torr, and (■) 4 Torr; solid lines represent the best fits.

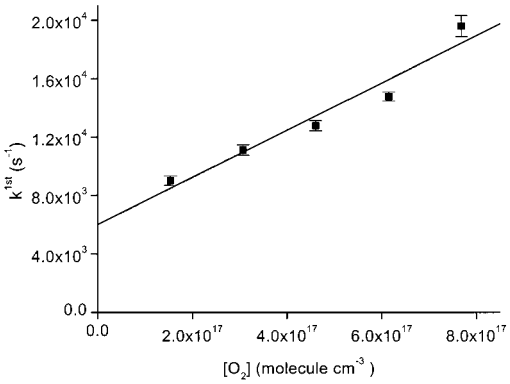

Figure 5. Plot of the pseudo-first-order rate constant versus the O_2 concentration at 251 K.

2. Reaction of 3-Pentoxy with O_2. The data for the rate of the O_2 reaction were analyzed in the same manner as the data for the NO reaction. Plots of the LIF signal versus the delay time are shown in Figure 4, and a plot of the pseudo-first-order rate constant versus the O_2 concentration is found in Figure 5. The intercepts of these plots increases from 6.9×10^3 to 1.7×10^4 s^{-1} as the temperature is raised from 220 to 285 K, respectively. The bimolecular reaction rate constant falls slightly from 1.8×10^{-14} to 1.25×10^{-14} cm^3 molecule^{-1} s^{-1} with increasing temperature. The temperature dependence of k_{O_2} is depicted in Figure 6. The resulting Arrhenius expression is

$$k_{O_2} = (4.10 \pm 1.24) \times 10^{-15} \exp[(2.65 \pm 0.63)\text{kJ mol}^{-1}/RT] \text{ cm}^3 \text{ molecule}^{-1} \text{ s}^{-1}$$

which can be extrapolated to $k_{O_2} = (1.2 \pm 0.6) \times 10^{-14}$ cm^3 molecule^{-1} s^{-1} at 298 K. Atkinson has proposed[3] that the rate constant for all secondary alkoxy radicals with O_2 is $k_{298K} = 8.0 \times 10^{-15}$ cm^3 molecule^{-1} s^{-1}, which is within the uncertainty of our data. Combined experimental and theoretical investigations performed by Hein et al.[9] suggested that the rate constant of 3-pentoxy with O_2 is $k_{O_2} = (7.2 \pm 3.5) \times 10^{-15}$ cm^3 molecule^{-1} s^{-1} at 298 K, which also is consistent with our result.

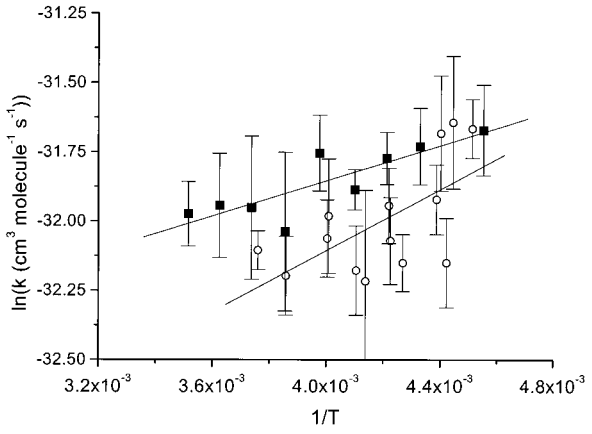

Figure 6. Arrhenius plot showing the temperature dependence of the rate constants for the reactions of 3-pentoxy with O_2 (■) and our present results for 2-butoxy + O_2 (○).

The effects of the experimental conditions were also checked by doubling the flow rates of all of the gases while keeping the partial pressures constant, resulting in a rate constant of $(1.7 \pm 0.1) \times 10^{-14}$ cm^3 molecule^{-1} s^{-1} versus $(1.8 \pm 0.3) \times 10^{-14}$ cm^3 molecule^{-1} s^{-1} at 219 K.

The antiparallel arrangement of the photolysis and probe laser beams in our previous kinetic study of 2-butoxy[24] created the potential for the accumulation of much higher concentrations of photochemical reaction products, and hence more unwanted chemistry, than does our current (perpendicular) arrangement of the two laser beams. The potential effects of unwanted chemistry are rather terrifying when one considers that the presence of 355 nm light, NO from RONO photolysis, and HO_2 produced in the RO + O_2 reaction can produce OH and O_3 via the same chemistry that produces O_3 in the polluted atmosphere:

$$HO_2 + NO \rightarrow OH + NO_2 \quad (2)$$

$$NO_2 + h\nu \rightarrow NO + O \quad (3)$$

$$O + O_2 + M \rightarrow O_3 + M \quad (4)$$

Our concern over the potential impact of secondary chemistry on our previous results led us to reinvestigate the 2-butoxy + O_2 reaction in the range 221 K $\leq T \leq$ 266 K. An Arrhenius plot of the results are shown in Figure 6, yielding a temperature dependence:

$$k_{2-\text{butoxy}+O_2} = (1.2 \pm 1.0) \times 10^{-15} \exp[(4.6 \pm 1.6)\ \text{kJ mol}^{-1}/RT]\ \text{cm}^3\ \text{molecule}^{-1}\ \text{s}^{-1}$$

which is consistent with our previous report of $k_{2-\text{butoxy}+O_2} = (1.3 \pm 0.4) \times 10^{-15} \exp[(5.5 \pm 0.7)\ \text{kJ mol}^{-1}/RT]$ cm^3 molecule^{-1} s^{-1}.[24] Two factors suggest a much greater influence of secondary chemistry on our previous work than on the present results: (1) the new rate constants are about 60% lower than the old values (although the results are consistent within the combined errors); (2) the intercepts of the plots of the pseudo-first-order rate constant versus [O_2] are about 6 times lower in the current arrangement than in our previous work (3.6×10^3 s^{-1} versus 2.2×10^4 s^{-1} at 277 K). We note that the intercepts of the pseudo-first-order plots are much larger for the O_2 reactions than for the NO reactions, and our previous results for 2-butoxy + NO appear to be valid (see Table 2).

The statistical uncertainties in our studies of alkoxy + O_2 reactions are very large, much larger than those in the alkoxy + NO reactions. This is largely because O_2 is an effective quencher of alkoxy radical fluorescence,[34] and the small value of the alkoxy + O_2 rate constant requires the use of fairly high O_2 concentrations. The effect of fluorescence quenching can be seen by studying how the intercepts of the plots of the LIF signal versus time (Figure 4) vary with the O_2 concentration and by comparing the intercepts to a similar plot for NO (Figure 1). As compared to the uncertainty generated by the poor S/N in the O_2 experiments, other sources of uncertainty would appear to contribute only modestly to the errors of most of the individual rate constants. The rate constant only varies by ~35% over the temperature range studied, so the error bars on the individual data points in Figure 6 imply a 2σ error in the activation energy for the 3-pentoxy reaction that approaches 100%. However, for the 2-butoxy + O_2 reaction, an error in E_a of similar magnitude still produces a definite negative temperature dependence.

TABLE 2: Rate Constants for the Reaction of 2-Butoxy with NO Compared to Those Computed from the Arrhenius Expression Derived in Our Previous Work[24]

temp (K)	previous results (calcd) (cm^3 molecule^{-1} s^{-1})	this work (cm^3 molecule^{-1} s^{-1})
276	$(2.7 \pm 0.9) \times 10^{-11}$	$(2.4 \pm 0.1) \times 10^{-11}$
253	$(3.1 \pm 0.8) \times 10^{-11}$	$(3.2 \pm 0.3) \times 10^{-11}$
226	$(3.7 \pm 0.6) \times 10^{-11}$	$(3.3 \pm 0.2) \times 10^{-11}$

Alkoxy radicals are generally assumed to react with O_2 via a bimolecular α-hydrogen abstraction reaction to form carbonyl compounds and hydroperoxy radicals:

$$CH_3CH_2CH(O\bullet)CH_2CH_3 + O_2 \rightarrow CH_3CH_2C(=O)CH_2CH_3 + HO_2 \quad (5)$$

For alkoxy radicals smaller than C_4, the reaction rate exhibits a positive temperature dependence (positive E_a), but our results for 3-pentoxy and, more strongly, 2-butoxy indicate a negative temperature dependence for the O_2 reactions.[24]

Jungkamp and Seinfeld investigated a mechanism for the reaction of alkoxy + O_2 reactions that could be used to rationalize a negative temperature dependence. Their quantum computations on the CH_3O + O_2 system suggested that the reaction was initiated by O_2 addition to the radical center to form a trioxy radical intermediate ($CH_3OOO\bullet$) that subsequently eliminates HO_2.[35] The addition reaction could possess a negative temperature dependence, and where this step is rate-limiting, one would expect to observe a negative temperature dependence. However, more recent calculations performed by Bofill et al.[36] indicate, fairly convincingly, that Jungkamp and Seinfeld misidentified the transition state. Bofill et al. find that the production of CH_2O + HO_2 from CH_3OOO would have to proceed via

$$CH_3OOO \rightarrow TS3 \rightarrow CH2OOH \rightarrow TS4 \rightarrow CH_2O + HO_2 \quad (6)$$

but that TS3 lies 51 kcal mol^{-1} above CH_3O + O_2, rendering this pathway inaccessible under atmospheric or even combustion conditions. Instead, the reaction is found to proceed via direct hydrogen abstraction through a cyclic structure involving "intermolecular noncovalent O−O bonding." Bofill et al. do find a weakly bound prereactive complex, albeit very different from a trioxy radical. A negative temperature dependence might be rationalized under conditions where this complex became important in the dynamics of the reaction. Note that such a complex would likely have a stronger influence at the subam-

TABLE 3: Arrhenius Parameters from Direct Studies of the Reaction of Alkoxy Radicals with O_2

radical	A (cm^3 $molecule^{-1}$ s^{-1})	E_a (kJ mol^{-1})	temp range (K)	ref
CH_3O	55×10^{-15}	8.3	298−450	12
C_2H_5O	71×10^{-15}	4.6	295−411	14
	24×10^{-15}	2.7	295−354	20
1-C_3H_7O	14×10^{-15}	0.9	223−303	17
	25×10^{-15}	2.0	289−381	20
2-C_3H_7O	10×10^{-15}	1.8	218−313	17
	15×10^{-15}	1.6	298−383	13
	16×10^{-15}	2.2	288−364	20
2-butoxy	1.33×10^{-15}	−5.5	223−311	24
	1.25×10^{-15}	−4.6	221−266	this work
3-pentoxy	4.10×10^{-15}	−2.6	220−285	this work

TABLE 4: Rate Constants for the Reaction of 3-Pentoxy with O_2 at 243 K at Different Total Pressures

total pressure (Torr)	k (cm^3 $molecule^{-1}$ s^{-1})	total pressure (Torr)	k (cm^3 $molecule^{-1}$ s^{-1})
50	$(1.42 \pm 0.10) \times 10^{-14}$	150	$(1.31 \pm 0.13) \times 10^{-14}$
100	$(1.44 \pm 0.18) \times 10^{-14}$		

bient temperatures used in our experiments rather than at the superambient temperatures of most, but not all, other alkoxy + O_2 experiments (see Table 3).

A negative temperature dependence implies the potential for the existence of a pressure dependence. Therefore, we investigated the pressure dependence of the rate constant at 243 K in the pressure range 50−150 Torr, but no obvious pressure dependence was found (see Table 4).

Balla et al. suggested that the activation energy for alkoxy + O_2 reactions was proportional to the C−H bond strength.[13] We therefore investigated the relative strength of the bond between the α-hydrogen and carbon atoms in 3-pentoxy versus 2-butoxy by calculating the energy of the isodesmic reaction

$$CH_3CH_2C(=O)CH_2CH_3 + CH_3CH(O\bullet)CH_2CH_3 \rightarrow CH_3CH_2CH(O\bullet)CH_2CH_3 + CH_3C(=O)CH_2CH_3 \quad (7)$$

The calculation was carried out using the Gaussian94[37] series of programs at the B3LYP/6-31G(d) and B3LYP/6-311G(2df, 2p) levels of theory; zero-point energies were determined at B3LYP/6-31G(d). The results indicate that the C−H bond strength for the α hydrogen is higher in 2-butoxy than in 3-pentoxy by 5.4 or 11.3 kJ mol^{-1} using the 6-31G(d) and 6-311G(2df, 2p) basis sets, respectively.

IV. Conclusion

Direct kinetic studies of the reactions of 3-pentoxy with NO and O_2 are carried out for the first time by using LIF to directly monitor the disappearance of 3-pentoxy radicals. Arrhenius expressions were obtained for both reactions. The rate constant for the reaction of 3-pentoxy with NO has a more-negative temperature dependence than those previously observed in smaller alkoxy radicals. The reactions of 3-pentoxy and 2-butoxy radicals with O_2 exhibit small-negative temperature dependencies. This is interesting in light of the small-positive temperature dependencies observed for ethoxy and propoxy radicals. The surprising temperature dependencies observed here for k_{NO} of the 3-pentoxy radical and k_{O_2} of both 2-butoxy and 3-pentoxy suggest that neither Arrhenius parameters nor 298 K rate constants for k_{NO} and k_{O_2} can be assumed to be independent of molecular size, even for radicals of very similar structure. It further suggests the need for direct kinetic studies of a much more diverse set of alkoxy radicals, not merely of those derived from linear alkanes. Further investigations of the pressure and temperature dependence of the rate of alkoxy radical + O_2 reactions would be invaluable for illuminating the dynamics of this important class of reactions.

Acknowledgment. The authors thank the National Science Foundation for support under Grant ATM-9712381. We thank C. Wang for his assistance in starting this project and B. S. Hudson for the loan of the hardware for data acquisition. We are also grateful for helpful discussions with S. Olivella and for the valuable comments of the referees.

References and Notes

(1) Sillman, S. *Atmos. Environ.* **1999**, *33*, 1821.
(2) Atkinson, R. *J. Phys. Chem. Ref. Data Monogr.* **1994**, *2*, 20−26.
(3) Atkinson, R. *Int. J. Chem. Kinet.* **1997**, *29*, 99.
(4) Somnitz, H.; Zellner, R. *Phys. Chem. Chem. Phys.* **2000**, *2*, 1899, 1907.
(5) Méreau, R.; Rayez, M. T.; Caralp, F.; Rayez, J. C. *Phys. Chem. Chem. Phys.* **2000**, *2*, 1919.
(6) Dibble, T. S. *J. Am. Chem. Soc.* **2001**, *123*, 4228.
(7) Hein, H.; Hoffmann, A.; Zellner, R. *Ber. Bunsen-Ges. Phys. Chem.* **1998**, *102*, 1840.
(8) Hein, H.; Hoffmann, A.; Zellner, R. *Phys. Chem. Chem. Phys.* **1999**, *1*, 3743.
(9) Hein, H.; Hoffmann, A.; Zellner, R. *Z. Phys. Chem. (Munich)* **2000**, *214*, 449.
(10) Sanders, N.; Butler, J. E.; Pasternack, L. R.; McDonald, J. R. *Chem. Phys.* **1980**, *48*, 203.
(11) Gutman, D.; Sanders, N.; Butler, J. E. *J. Phys. Chem.* **1982**, *86*, 66.
(12) Lorenz, K.; Rhäsa, D.; Zellner, R.; Fritz, B. *Ber. Bunsen-Ges. Phys. Chem.* **1985**, *89*, 341.
(13) Balla, R. J.; Nelson, H. H.; McDonald, J. R. *Chem. Phys.* **1985**, *99*, 323.
(14) Hartmann, D.; Karthäuser, J.; Sawerysyn, J. P.; Zellner, R. *Ber. Bunsen-Ges. Phys. Chem.* **1990**, *94*, 639.
(15) Frost, M. J.; Smith, I. W. M. *J. Chem. Soc., Faraday Trans.* **1990**, *86*, 1757.
(16) Frost, M. J.; Smith, I. W. M. *J. Chem. Soc., Faraday Trans.* **1990**, *86*, 1751.
(17) Mund, C.; Fockenberg, C.; Zellner, R. *Ber. Bunsen-Ges. Phys. Chem.* **1998**, *102*, 709.
(18) Devolder, P.; Fittschen, Ch.; Frenzel, A.; Hippler, H.; Poskrebyshev, G.; Striebel, F.; Viskolcz, B. *Phys. Chem. Chem. Phys.* **1999**, *1*, 675.
(19) Caralp, F.; Devolder, P.; Fittschen, C.; Gomz, N.; Hippler, H.; Méreau, R.; Rayez, M. T.; Striebel, F.; Viskolcz, B. *Phys. Chem. Chem. Phys.* **1999**, *1*, 2935.
(20) Fittschen, C.; Frenzel, A.; Imrik, K.; Devolder, P. *Int. J. Chem. Kinet.* **1999**, *31*, 860.
(21) Blitz, M.; Pilling, M. J.; Robertson, S. H.; Seakins, P. W. *Phys. Chem. Chem. Phys.* **1999**, *1*, 73.
(22) Wang, C. J.; Shemesh, L. G.; Deng, W.; Lilien, M. D.; Dibble, T. S. *J. Phys. Chem. A* **1999**, *103*, 8207.
(23) Wang, C. J.; Deng, W.; Shemesh, L. G.; Lilien, M. D.; David, R. K.; Dibble, T. S. *J. Phys. Chem. A* **2000**, *104*, 10368.
(24) Deng, W.; Wang, C. J.; Katz, D. R.; Gawinski, G. R.; Davis, A. J.; Dibble, T. S. *Chem. Phys. Lett.* **2000**, *330*, 541.
(25) Fittschen, C.; Hippler, H.; Viskolcz, B. *Phys. Chem. Chem. Phys.* **2000**, *2*, 1677.
(26) Lotz, C.; Zellner, R. *Phys. Chem. Chem. Phys.* **2000**, *2*, 2353.
(27) Lotz, C.; Zellner, R. *Phys. Chem. Chem. Phys.* **2001**, *3*, 2607
(28) Carter, C. C.; Atwell, J. R.; Gopalakrishnman, S.; Miller, T. A. *J. Phys. Chem. A* **2000**, *104*, 9165.
(29) Carter, C. C.; Gopalakrishnman, S.; Atwell, J. R.; Miller, T. A. *J. Phys. Chem. A* **2001**, *105*, 2925.
(30) Blatt, A. H. *Organic Synthesis*; Wiley: New York, 1966; pp 108−109.
(31) For typical alkyl nitrite IR and NMR spectra, see: *Sadtler Index*; Bio-Rad Laboratories Inc: Philadelphia, PA, 1973.
(32) For typical alkyl nitrite UV spectra, see: Calvert, J. G.; Pitts, J. N., Jr.; *Photochemistry*; Wiley: New York, 1966.
(33) Caralp, F.; Rayez, M.-T.; Forst, W.; Gomez, N.; Delcroix, B.; Fittschen, C.; Devolder, P. *J. Chem. Soc., Faraday Trans.* **1998**, *94*, 3321.

(34) Lin, S. R.; Lee, Y. P.; Nee, J. B. *J. Chem. Phys.* **1988**, *88*, 171.
(35) Jungkamp, T. P. W.; Seinfeld, J. H. *Chem. Phys. Lett.* **1996**, *263*, 371.
(36) Bofill, J. M.; Olivella, S.; Solé, A.; Anglada, J. M. *J. Am. Chem. Soc*. **1999**, *121*, 1337.
(37) Frisch, M. J.; Trucks, G. W.; Schlegel, H. B.; Gill, P. M. W.; Johnson, B. G.; Robb, M. A.; Cheeseman, J. R.; Keith, T.; Petersson, G. A.; Montgomery, J. A.; Raghavachari, K.; Al-Laham, M. A.; Zakrzewski, V. G.; Ortiz, J. V.; Foresman, J. B.; Cioslowski, J.; Stefanov, B. B.; Nanayakkara, A.; Challacombe, M.; Peng, C. Y.; Ayala, P. Y.; Chen, W.; Wong, M. W.; Andres, J. L.; Replogle, E. S.; Gomperts, R.; Martin, R. L.; Fox, D. J.; Binkley, J. S.; Defrees, D. J.; Baker, J.; Stewart, J. P.; Head-Gordon, M.; Gonzalez, C.; Pople, J. A. *Gaussian94*, Revision D.3; Gaussian, Inc.: Pittsburgh, PA, 1995.